

Reliable Iterative RTO of a Continuously Operated Hydroformylation Process

Reinaldo Hernández* Jens Dreimann** Sebastian Engell*

* *Process Dynamics and Operations Group, TU Dortmund, Emil-Figge-Str. 70, 44227 Dortmund, Germany (e-mail: {reinaldo.hernandez, sebastian.engell}@bci.tu-dortmund.de).*

** *Laboratory of Chemical Process Development, TU Dortmund, Emil-Figge-Str. 66, 44227 Dortmund, Germany (e-mail: {jens.dreimann}@tu-dortmund.de).*

Abstract: In this work, the application of a reliable iterative real-time optimization (RTO) scheme to a continuously operated transition metal complex catalyzed process for the hydroformylation of 1-dodecene is presented. The aim of the proposed scheme is to ensure optimal operation despite the presence of model uncertainties and measurement errors. Iterative optimization using Modifier Adaptation with Quadratic Approximation (MAWQA) is applied. Furthermore, additional modules for steady-state identification (SSI) and robust data reconciliation (DR) were designed and implemented. The proposed scheme was commissioned in a real miniplant, and a significantly improved performance in comparison to the optimal operating point that was obtained from the nominal process model was achieved.

Keywords: Real-Time Optimization, Plant-model Mismatch, Modifier Adaptation, Experimental Validation.

1. INTRODUCTION

The study of transition metal complex catalysis is one of the most active research fields in industrial chemistry due to the insurmountable high selectivity and activity that can be attained at mild reaction conditions in comparison to the heterogeneous counterpart. Furthermore, due to the minimization of waste and saving of energy, transition metal complex catalysis has been identified as one of the key technologies in green chemistry, whose relevance is illustrated by the fact that during the last two decades, three Nobel prizes in chemistry (2001, 2005, 2010) have been awarded to researchers working in this field (Behr and Neubert, 2012). However, commercial applications of transition metal complex catalysis are still relatively limited, which can be mainly explained by the high prices of the required metals and ligands. This leads to the need for highly efficient catalyst recovery concepts and a careful selection of the operating conditions (Dreimann et al., 2016).

The traditional way to address the economically optimal operation of chemical process has been the use of Real-time Optimization. The idea is to make use of a stationary (usually first principles based) nonlinear model of the process in order to compute the set-points that maximize the economic performance of the plant while different environmental, safety and process constraints are satisfied. In the conventional two-step approach, the available plant

measurements are used to update a subset of the model parameters with the aim of operating the process as close as possible to the actual optimum. Unfortunately, there are numerous limitations to this approach including the proper selection of the parameters to be updated, their identifiability and the fact that under the presence of structural plant-model mismatch, convergence to the actual optimum cannot be ensured or even worse it might steer the process to an operating point where the constraints are violated (Chachuat et al., 2009).

In order to address the issue of structural plant-model mismatch and to overcome the aforementioned difficulties of online parameters estimation, the addition of bias and gradient correction terms to the nominal optimization problem has been proposed in the so-called Modifier Adaptation (MA) framework (Tatjewski, 2002; Gao and Engell, 2005; Marchetti et al., 2016). The methodology has been widely investigated during the last years due to its ability to converge to the plant optimum under relatively mild assumptions regarding the quality of the available process model. The main challenge during the implementation of MA is the accurate estimation of the plant gradients. The use of finite difference was proposed in the seminal work of Roberts (Roberts, 1979), which limits the application of the method to low-dimensional problems with low noise levels. During the last few years, different approaches have been proposed in order to address the issue of accurate estimation of the plant gradients, including dual modifier adaptation (Dual-MA) (Marchetti et al., 2010), Nested Modifier Adaptation (Navia et al., 2015), and the use of quadratic surrogate models in Modifier Adaptation with quadratic Approximation (MAWQA) (Gao et al., 2016b).

* This work is part of the Collaborative Research Center "Integrated Chemical Processes in Liquid Multiphase Systems" - InPROMPT. Financial support by the Deutsche Forschungsgemeinschaft (DFG) is gratefully acknowledged (TR63)

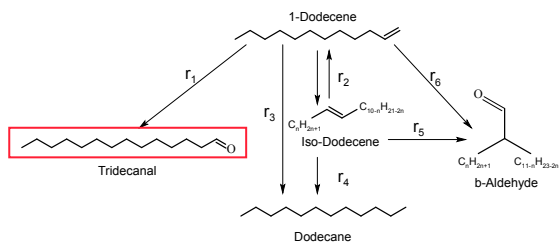


Fig. 1. Reaction network for the case study hydroformylation of 1-Dodecene in a TMS system

In this work, a RTO scheme was developed and tested on miniplant scale for a transition metal complex catalyzed process. In order to deal with plant-model mismatch, a reliable iterative optimization scheme based on MAWQA was designed. Furthermore, additional modules to handle measurements errors were developed.

2. CASE STUDY: HYDROFORMYLATION OF 1-DODECENE IN A TMS SYSTEM

2.1 Process Description

Hydroformylation is one of the best known applications of transition metal catalysis used in industry on a large scale for the production of aldehydes by reaction of alkenes with syngas (CO/H₂) (Behr and Neubert, 2012). It has been widely studied as a model reaction due to its similarities to other processes such as hydroesterification, hydrocarbonylation, hydroaminomethylation and hydrosilylation. Furthermore, hydroformylation has been proposed as a key step for the functionalization and processing of renewable raw materials as e.g. fatty oils.

The reaction takes place in the presence of a rhodium complex that is produced by the reaction of the precursor (acetylacetonato) - dicarbonylrhodium(I) Rh(acac)(CO)₂ and the ligand BiPhePhos. The reaction network is presented in Figure 1. Besides the main reaction i.e. the hydroformylation of 1-dodecene to tridecanal, several side-reactions take place, leading to the formation of different side products: isomers of 1-dodecene (lumped as *iso*-dodecene), branched aldehydes (*b*-aldehyde) and isomers of dodecane. In order to ensure an efficient recovery of the expensive catalyst, the reaction takes place in a thermoregulated multicomponent solvent (TMS) system. A careful selection of a non-polar and a polar solvent ensures a single liquid phase at reaction conditions, while after cooling down the reaction mixture, the non-polar product phase is separated from the catalyst rich polar phase which can be recycled to the reactor. In the case of the hydroformylation of 1-Dodecene, the TMS system 50/50, %m/%m mixture of the non-polar solvent *n*-decane and the polar solvent *N,N*-Dimethylformamide (DMF) has been proposed. It has been shown that this system yields high conversion and selectivity with low catalyst leaching (Brunsch and Behr, 2013).

The process concept has been successfully demonstrated on miniplant scale (Zagajewski et al., 2014). In Figure 2, a simplified flow diagram of the miniplant is presented. The substrate 1-dodecene is fed together with the non-polar solvent *n*-Decane (vessel **B1** via **P1**) and the polar solvent DMF (vessel **B2** via **P2**) to the reactor **B3**. Dissolved

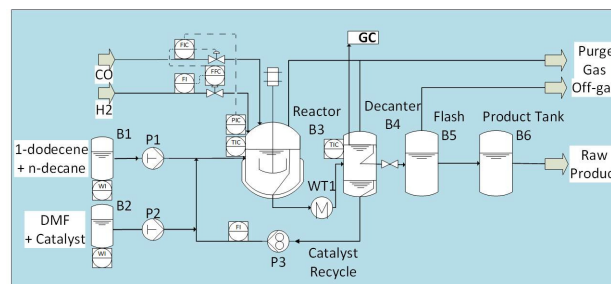


Fig. 2. Simplified flowsheet of the miniplant used as case study in this work

catalyst **B2** is also replenished to the system. The reactor **B3** consists of a 1000 ml vessel with a constant liquid holdup of 300 ml. A constant temperature is kept in the reactor by heat exchange with the jacket. Carbon monoxide and hydrogen are fed to the reactor **B3** under pressure and ratio control. After leaving **B3**, heat is removed from the reaction mixture in the heat exchanger **WT1**. In the decanter **B4**, the non-polar (product) and the polar (catalyst) phases are separated. The catalyst phase is pumped back to the reactor via pump **P3** while the product phase is sent to further processing. The product is analyzed online by gas chromatography (GC) by sampling the non-polar phase in **B4**.

2.2 Model Description

In this section a brief description of the process model is given. Further details can be found in previous works (Hernandez and Engell, 2016; Gao et al., 2016a). According to the material balance, the amounts (in mol) of the different liquid components $n_{i,\text{liquid}}$ ($i = n$ -dodecene, tridecanal, dodecane, etc) in the reactor liquid phase are given by (1):

$$\frac{dn_{i,\text{liquid}}}{dt} = 0 = \dot{n}_{i,\text{in}} - \dot{n}_{i,\text{out}} + M_{\text{cat}} \sum_{l=1}^{N_l} \nu_{i,l} r_l, \quad (1)$$

where M_{cat} is the mass of active catalyst in the reactor and $\dot{n}_{i,\text{in}}, \dot{n}_{i,\text{out}}$ are molar inflow and outflow rate of the component i . $\nu_{i,l}$ are the coefficients of the stoichiometric matrix for the liquid component i and r_l is the reaction rate for the l reaction. For hydrogen and carbon monoxide, the material balance (1) is extended to include the molar flux J_j of the gas component j from the gas phase to the liquid phase:

$$\frac{dn_{j,\text{liquid}}}{dt} = 0 = J_j a V_{R,\text{liquid}} - \dot{n}_{j,\text{out}} + M_{\text{cat}} \sum_{l=1}^{N_l} \nu_{j,l} r_l, \quad (2)$$

where a is the G-L interfacial area per unit volume. The two-film theory is used for the description of the mass transfer in the G-L interface. After introducing the overall mass transfer coefficients ($k_{j,G}$) based on the difference between the bulk concentration in one phase $C_{j,\text{liquid}}^{\text{bulk}}$ and the concentration that would be in equilibrium ($C_{j,\text{liquid}}^{\text{eq}}$) with the bulk concentration in the other phase, the flux is computed as:

$$J_j = k_{j,G} \left(C_{j,\text{liquid}}^{\text{eq}} - C_{j,\text{liquid}}^{\text{bulk}} \right), \quad (3)$$

with the equilibrium concentration given by:

$$C_{j,\text{liquid}}^{\text{eq}} = \frac{\frac{1}{RT_{\text{Reactor}}} \frac{V_{R,\text{gas}}}{V_{R,\text{liquid}}} p_j + C_{j,\text{liquid}}^{\text{bulk}}}{\frac{1}{RT_{\text{Reactor}}} \frac{V_{R,\text{gas}}}{V_{R,\text{liquid}}} H_j + 1}, \quad (4)$$

where H_j is the Henry coefficient. Further details regarding the kinetic model (expression of the reaction rate r_l) can be found in (Kiedorf et al., 2014), (Hentschel et al., 2015). It is assumed that the LLE between the phases is reached in the decanter. Based on experimental values, simple expressions of the equilibrium constants K_i as functions of the decanter temperature for all the liquid components i were obtained:

$$K_i = \exp\left(A_{i,0} + \frac{A_{i,1}}{T_{\text{decanter}}} + A_{i,2}T_{\text{decanter}}\right), \quad (5)$$

where $A_{i,0}$, $A_{i,1}$ and $A_{i,2}$ are parameters obtained by regression of experimental data. The split factor ζ_i and the molar flows of the components in the product stream ($\dot{n}_{i,\text{product}}$) and of the catalyst stream ($\dot{n}_{i,\text{catalyst}}$) as a function of the inlet flow to the decanter ($\dot{n}_{i,\text{decanter}}$) can be computed by:

$$\dot{n}_{i,\text{product}} = \zeta_i \dot{n}_{i,\text{decanter}}; \quad (6a)$$

$$\dot{n}_{i,\text{catalyst}} = (1 - \zeta_i) \dot{n}_{i,\text{decanter}} \quad \zeta_i = \frac{K_i}{1 + K_i}. \quad (6b)$$

As was stated in equation (1) the reaction rate is proportional to the mass of the active catalyst $M_{\text{cat}} = C_{\text{cat}} V_{R,\text{liquid}}$. At high carbon monoxide concentrations, catalyst deactivation can take place by formation of inactive species as Rh-di-carbonyl and Rh-dimer. This phenomenon has been approximately quantified by Hentschel et al. (2015) according to:

$$C_{\text{cat}} = \frac{C_{\text{Rh-precursor,liquid}}^{\text{bulk}}}{1 + K_{\text{cat},1} C_{\text{CO,liquid}}^{\text{bulk}} + K_{\text{cat},2} \frac{C_{\text{CO,liquid}}^{\text{bulk}}}{C_{\text{H}_2,\text{liquid}}^{\text{bulk}}}}. \quad (7)$$

The active catalyst concentration C_{cat} is expressed as a function of the Rh-precursor concentration $C_{\text{Rh-precursor}}$ and the CO and H₂ concentrations in the liquid phase. The constants $K_{\text{cat},1}$ and $K_{\text{cat},2}$ account for uncertainty in the catalyst pre-equilibrium. The product composition predicted by the model was compared to experimental data and a root-mean-square error of 2.47 % was observed.

3. PROPOSED OPTIMIZATION SCHEME

A simplified block diagram of the proposed RTO scheme is shown in figure 3. It is similar to the typical structure used in commercial RTO systems based on the two-step approach (Camara et al., 2016). However, instead of including a parameter estimation step, the model uncertainties are addressed via Modifier Adaptation with Quadratic Approximation. Moreover, steady-state identification (SSI) and robust data reconciliation (DR) blocks have been implemented in order to provide robustness under measurements errors. The execution of the RTO layer can be triggered when a steady-state has been detected based on the raw data (GC analysis, temperature, flow rates, pressure). The raw data is processed by the DR module and used to estimate the objective function that is used by the iterative optimization algorithm. Finally, the iterative optimization module computes the set points that are implemented by the regulatory control layer.

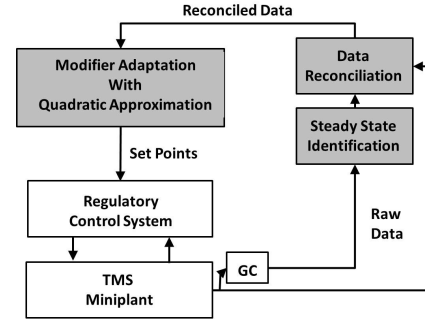


Fig. 3. Block diagram of the proposed RTO scheme

The miniplant is connected to a control computer that runs a LabVIEW application. A sample of the product in the decanter is taken automatically by the GC analyzer. The signal is sent to a second computer where the raw data is processed to estimate the current product composition. A TCP/IP protocol suite was chosen to realize the communication between the system components.

3.1 Steady State Identification

An F -statistical test is used in order to perform an automatic identification of a steady state. The basic idea is to compare the variance of the raw data with the variance obtained from the filtered data at each sampling point (Cao and Russell, 1995). As a result, a fast detection of stationaryity is obtained. Despite its simplicity, relatively good accuracy of the detection of steady states has been reported in different works. After defining the filter constants $0 < \lambda_1, \lambda_2, \lambda_3 < 1$ The raw data y^i is analyzed according to:

- **Step 1:** y^i is filtered ($y^{i,f}$) by using an exponential moving average filter $y^{i,f} = \lambda_1 y^i + (1 - \lambda_1) y^{i-1,f}$
- **Step 2:** The filtered square deviation $(v^{i,f})^2$ is calculated according to:
$$(v^{i,f})^2 = \lambda_2 (y^i - y^{i-1,f})^2 + (1 - \lambda_2) (v^{i-1,f})^2$$
- **Step 3:** The filtered square difference $(d^{i,f})^2$ of successive data is computed by:
$$(d^{i,f})^2 = \lambda_3 (y^i - y^{i-1})^2 + (1 - \lambda_3) (d^{i-1,f})^2$$
- **Step 4:** Finally, the R statistic defined by the ratio between the previously calculated variances $R = \frac{(2 - \lambda_1)(v^{f,i})^2}{(d^{f,i})^2}$ is evaluated.

The obtained value of R is compared with a critical value R_{crit} . If $R > R_{\text{crit}}$ then the process is considered not to be at steady state at the corresponding level of significance. In our case study, the composition measurements from the GC (mass fraction w_i) are used to identify the stationarity of the complete process.

3.2 Robust Data Reconciliation

Due to the presence of noise and gross errors in the collected data, the material balance in the miniplant might not be satisfied. In order to overcome this issue, a Data Reconciliation (DR) module was designed. The basic idea is to adjust the collected data in such a way that the reconciled values satisfy the material balance. Specifically, for our case study, the material balances of the polar

and the non-polar solvent must be satisfied at steady state. Furthermore, despite the assumption that there are uncertainties in the kinetic model, the total molar inflow of the substrate to the miniplant should be the same as the sum of the molar outflow of the different species that take part in the reaction network. The DR problem for the Miniplant is formulated as:

$$\begin{aligned} \max_{\mathbf{d}} \quad & \sum \rho(\xi_i) \\ \text{s.t.} \quad & \dot{n}_{DMF,1} = \dot{n}_{DMF,3}; \\ & \dot{n}_{n-Decane,1} = \dot{n}_{n-Decane,3} \\ & \dot{n}_{1-Dodecene,1} = \dot{n}_{1-Dodecene,3} + \dot{n}_{Iso-Dodecene,3} \dots \\ & + \dot{n}_{tridecanal,3} + \dot{n}_{b-Aldehyde,3} + \dot{n}_{dodecane,3}, \end{aligned} \quad (8)$$

where $\xi_i = w_i - \hat{w}_i$ is the estimation error. The decision variables \mathbf{d} of the problem are the reconciled mass flow of the pumps **P1** and **P2** and the reconciled mass fractions (\hat{w}_i) in the product streams. For a robust estimation in case of outliers, the traditional least square objective function was replaced by a Welsch estimator defined by:

$$\rho(\xi_i, c_w) = \frac{c_w^2}{2} \left(1 - \exp \left(- \left(\frac{\xi_i}{c_w} \right)^2 \right) \right) \quad (9)$$

with tuning parameter c_w . A value of $c_w = 2.9846$ is used to obtain 95% asymptotic efficiency on the standard distribution (Korpela et al., 2016).

3.3 Modifier Adaptation with Quadratic Approximation

The nominal optimization problem can be stated as:

$$\begin{aligned} \min_{\mathbf{u}} \quad & J_m(\mathbf{u}) \\ \text{s.t.} \quad & \mathbf{C}_m(\mathbf{u}) \leq 0 \\ & \mathbf{u}^{lb} \leq \mathbf{u} \leq \mathbf{u}^{ub}, \end{aligned} \quad (10)$$

where $\mathbf{u} \in \mathbb{R}^{n_u}$ is a vector of manipulated plant inputs bounded by \mathbf{u}^{lb} and \mathbf{u}^{ub} , $J_p(\mathbf{u}): \mathbb{R}^{n_u} \rightarrow \mathbb{R}$ is a scalar objective function (economic performance index), and $\mathbf{C}_p(\mathbf{u}): \mathbb{R}^{n_u} \rightarrow \mathbb{R}^{n_c}$ is the vector of plant constraints and model equations; the objective function and the constraints are assumed to be twice differentiable. To deal with plant-model mismatch, MA introduces bias and gradients correction terms (modifiers) to (10), which results in a problem that is solved iteratively (Gao and Engell, 2005):

$$\begin{aligned} \min_{\mathbf{u}} \quad & J_{ad}^{(k)}(\mathbf{u}) := J_m(\mathbf{u}) + \epsilon_J^{(k)} + \lambda_J^{(k)} \left(\mathbf{u} - \mathbf{u}^{(k)} \right) \\ \text{s.t.} \quad & \mathbf{C}_{ad}^{(k)}(\mathbf{u}) := \mathbf{C}_m(\mathbf{u}) + \epsilon_C^{(k)} + \lambda_C^{(k)} \left(\mathbf{u} - \mathbf{u}^{(k)} \right) \leq 0 \\ & \mathbf{u}^{lb} \leq \mathbf{u} \leq \mathbf{u}^{ub}, \end{aligned} \quad (11)$$

with the superscript k denoting the iteration number. The bias is corrected by the zeroth-order modifiers ϵ , and the gradient correction is done by the first-order modifiers λ :

$$\begin{aligned} \epsilon_J^{(k)} &= J_p^{(k)} - J_m^{(k)}; \epsilon_C^{(k)} = \mathbf{C}_p^{(k)} - \mathbf{C}_m^{(k)} \\ \lambda_J^{(k)} &= \left(\nabla J_p^{(k)} - \nabla J_m^{(k)} \right)^T; \lambda_C^{(k)} = \left(\nabla \mathbf{C}_p^{(k)} - \nabla \mathbf{C}_m^{(k)} \right)^T, \end{aligned} \quad (12)$$

where the subscripts p and m denote the plant and the model.

As stated before, the main challenge is the estimation of the plant gradients. In this work Modifier Adaptation

with Quadratic Approximation (MAWQA) is used as a key element in the proposed robust RTO scheme. The idea behind of the algorithm is the estimation of the plant gradients by fitting a quadratic model to the data that was obtained at previous set-points. This is illustrated below for the objective function, the same procedure is applied for the approximation of the constraints. The quadratic approximation of the cost function is defined by:

$$J_\phi(\mathbf{u}, \boldsymbol{\theta}) = \sum_{i=1}^{n_u} \sum_{j=1}^i a_{i,j} u_i u_j + \sum_{i=1}^{n_u} b_i u_i + c, \quad (13)$$

with the parameter set $\boldsymbol{\theta} = \{a_{1,1}, \dots, a_{n_u, n_u}, b_1, \dots, b_{n_u}, c\}$ obtained from solving the least-squares problem:

$$\min_{\boldsymbol{\theta}} \sum_{i=1}^{n_r} \left(J_p(\mathbf{u}^{(r_i)}) - J_\phi(\mathbf{u}^{(r_i)}, \boldsymbol{\theta}) \right)^2, \quad (14)$$

where $\mathbf{u}^{(r_i)}$ are the elements of the regression set $\mathcal{U}^{(k)}$ composed of past set-points selected to guarantee well-posedness of problem. The regression set $\mathcal{U}^{(k)} = \mathcal{U}_{nb}^{(k)} \cup \mathcal{U}_{dist}^{(k)}$ include the set of points within the neighborhood of the current iteration $\mathcal{U}_{nb}^{(k)}$ (i.e. within a ball of predefined size) and the set of distant distant points $\mathcal{U}_{dist}^{(k)}$ according to:

$$\begin{aligned} \min_{\mathcal{U}_{dist}^{(k)}} \quad & \frac{\sum \|\mathbf{u} - \mathbf{u}^{(k)}\|}{\phi(\mathcal{U}_{dist}^{(k)})} \\ \text{s.t.} \quad & \text{size}(\mathcal{U}_{dist}^{(k)}) = (n_u + 1)(n_u + 2)/2 - 1 \end{aligned} \quad (15)$$

where $\phi(\mathcal{U}_{dist}^{(k)})$ is the minimal angle between all the possible pair of vectors of the regression set. After the quadratic model has been built, it is assumed that $\nabla J_p^{(k)} \approx \nabla J_\phi^{(k)}$, based on the fact that the quadratic model locally captures first and second order information of the actual (unknown) plant map. Due to the restricted (local) validity of the previous approximation, the new set-point obtained from the iteration on (15) is constrained to be within a trust-region that can be adapted after each iteration ($\|\mathbf{u}^{(k+1)} - \mathbf{u}^{(k)}\| \leq \Delta^{(k)}$). The rate of convergence is affected by the value of the initial perturbations and the size of the trust region. The optimal values of those parameters which increase the rate of convergence are not known a priori but can be tuned by using simulations.

Furthermore, the strategy proposed by Gao et al. (2016b) includes the possibility of directly using the quadratic approximation instead of the modified problem according to the prediction accuracies of the models. A detailed description of the algorithm can be found in (Gao et al., 2016b).

4. PROBLEM FORMULATION

The RTO problem is formulated as the maximization of the product yield ($Y_{tridecanal}$), subject to the model equations, input bounds and process constraints, represented by the map $\mathbf{C}(\mathbf{u})$.

$$\begin{aligned} \max_{\mathbf{u}} \quad & J = Y_{tridecanal}(\mathbf{u}) \\ \text{s.t.} \quad & \mathbf{C}(\mathbf{u}) \leq 0 \\ & \mathbf{u}^{lb} \leq \mathbf{u} \leq \mathbf{u}^{ub}. \end{aligned} \quad (16)$$

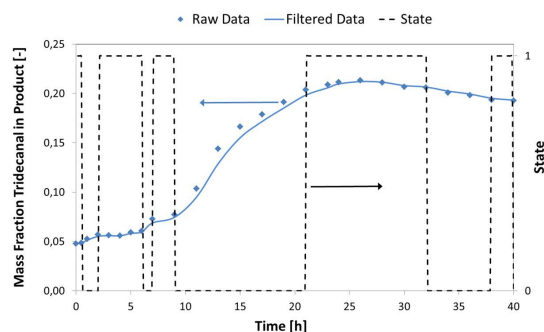


Fig. 4. Performance of the steady state identification algorithm with real plant data

As degrees of freedom (\mathbf{u}), the set-points of the following controlled variables are considered: reactor temperature ($85^{\circ}\text{C} \leq T_{\text{Reactor}} \leq 105^{\circ}\text{C}$), reactor pressure ($10\text{bar} \leq P_{\text{Reactor}} \leq 30\text{bar}$), molar fraction of carbon monoxide in feed gas ($0.1 \leq y_{\text{CO}} \leq 0.9$), catalyst dosing ($0.1\text{ppm} \leq \dot{n}_{\text{catalyst,in}} \leq 4\text{ppm}$) and decanter temperature ($5^{\circ}\text{C} \leq T_{\text{decanter}} \leq 15^{\circ}\text{C}$).

5. RESULTS

Due to space limitation, the scope of this paper is restricted to the validation of the scheme. The reader is referred to previous works involving simulation studies (Hernandez and Engell, 2016), (Gao et al., 2016a).

5.1 Steady State Identification

Historical data from miniplant experiments were used to validate the algorithm. Figure 4 displays the results of the SSI algorithm for data collected during the start-up of the miniplant with parameters $\lambda_1 = 0.70$, $\lambda_2 = 0.95$, $\lambda_3 = 0.63$ and $R_{\text{crit}} = 2.0$. In the primary vertical axis (left), the raw and filtered data regarding the mass fraction of tridecanal in the product phase is presented, while the secondary axis (right) is used for indicating the state of the system. A value of state=1 corresponds to the case that the process is stationary while state=0 represents a transition state. As can be observed, the algorithm is able to reliably distinguish between transients and stationary states despite the simplicity of the proposed approach.

5.2 Robust Data Reconciliation

The DR scheme described in section 3.2 was also validated with historical data. Table 1 illustrates the performance of the approach by comparing the material balance before and after data reconciliation for a particular stationary operating point. As can be observed, a significant difference between the raw data and the reconciled data is observed for the flow of DMF. This can be associated to errors during the calibration of the pump **P2**. Minor adjustments are made to the composition measured by the GC. As a result, a consistent material balance is obtained that is used in the online computation of the objective function.

5.3 Iterative Set-Point Optimization

Preliminary simulation studies showed that for different uncertainty scenarios, the decanter temperature is kept

Table 1. Material balance for the Miniplant

Component	Raw Flow [g/h]		Rec. Flow [g/h]	
	Inlet	Outlet	Inlet	Outlet
DMF	4.25	3.27	2.55	2.55
Decane	32.08	30.72	32.08	32.08
1-Dodecene	12.22	1.74	12.22	1.73
Iso-Dodecene	0	2.72	0	2.70
Dodecane	0	0.05	0	0
b-Aldehyde	0	0.38	0	0.37
Tridecanal	0	8.86	0	9.09

always at its minimum while the total pressure is kept at the maximum value. This can be explained by the fact that at a low temperature in the decanter the catalyst leaching is minimized, while the increase of the pressure leads to an increase in the reaction rate that can compensate a lower catalyst concentration. Furthermore, changes in the catalyst dosing lead to an extremely slow transition between steady states, a problem that will be addressed in another work. Therefore, in this work the problem is simplified by considering only the molar fraction of carbon monoxide in the feed gas and the reactor temperature as decision variables in the iterative optimization scheme, while the rest of the variables are kept at the optimum that was computed by using the nominal model.

Figure 5 shows the trajectory of the yield of tridecanal before and after implementation of the closed-loop RTO scheme. As can be seen the algorithm generates a series of inputs that lead to an improvement of the tridecanal yield from 73.3% at the nominal optimum to a final value of 76.6% after 40 hours, equivalent to 7 iterations. Figure 6 shows the trajectory of the manipulated variables, the reactor temperature is adjusted from the initial value of 95°C to 105°C while the molar fraction of CO is adjusted from the original value of 0.50 to the final value of 0.68. The increase of temperature improves the selectivity towards the desired product that can be explained by the difference of the activation energies between the reactions. On the other hand, the adjustment of the molar fraction of CO affects the concentration of active catalyst in the reaction medium as well as the concentration of CO in the bulk liquid itself. It has been reported in previous works, that the partial pressure of CO has a significant influence on the performance of the reaction. A low partial pressure leads to a lower concentration in the liquid phase with a detrimental effect in the hydroformylation reactions, but high partial pressure might lead to catalyst deactivation. The influence of the new operating point on the yield of the side products is displayed in Figure 7. As can be seen, the final operating point leads to a higher rate of all the hydroformylation reactions including the formation of branched aldehyde.

6. CONCLUSIONS

In this work, an improved operation of a continuously operated transition metal catalyzed hydroformylation process has been achieved by means of a reliable Real-time Optimization scheme which is able to handle model uncertainty and measurement errors. The proposed scheme has been validated in a miniplant for the model reaction hydroformylation of 1-Dodecene in a thermoregulated multicomponent (TMS) solvent system. Future work will

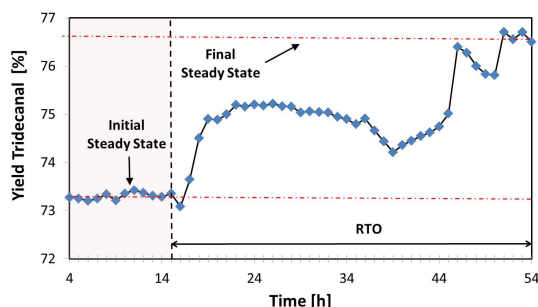


Fig. 5. Trajectory of the yield of tridecanal before and after application of the proposed RTO scheme

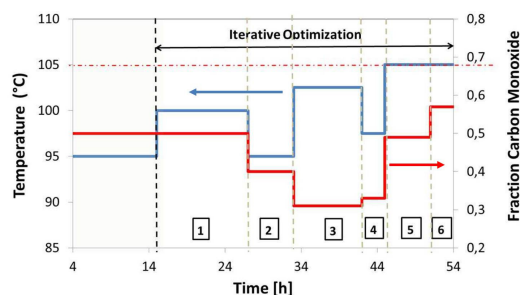


Fig. 6. Trajectory of the manipulated variables: reactor temperature and molar fraction of CO in the gas feed.

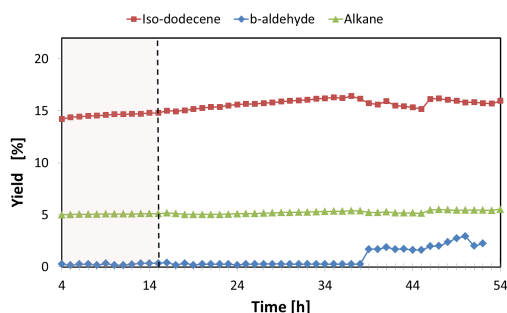


Fig. 7. Yields of dodecane, b-aldehyde and iso-dodecene

incorporate recent developments on the use of transient information for a faster convergence to the optimal operating point (Gao et al., 2017).

REFERENCES

Behr, A. and Neubert, P. (2012). *Applied Homogeneous Catalysis*. Wiley-VCH.

Brunsch, Y. and Behr, A. (2013). Temperature controlled catalyst recycling in homogeneous transition-metal catalyst: minimization of catalyst leaching. *Ang. Chem. Int. Ed.*, 52, 1586–1589.

Camara, M., Quelhas, A., and Pinto, J. (2016). Performance evaluation of real industrial rto systems. *Processes*, 4(44). doi:10.3390/pr4040044.

Cao, S. and Russell, R. (1995). An efficient method for on-line identification of steady state. *J. Process Control*, 5(6), 363–374.

Chachuat, B., Srinivasan, B., and Bonvin, D. (2009). Adaptation strategies for real-time optimization. *Comput. Chem. Eng.*, 33, 1557–1567.

Dreimann, J., Lutze, P., Zagajewski, M., Behr, A., Gorak, A., and Vorholt, A. (2016). Highly integrated reactor-separator systems for the recycling of homogeneous catalysis. *Chem. Eng. Process.*, 99, 124–131.

Gao, W. and Engell, S. (2005). Iterative set-point optimization of batch chromatography. *Comput. Chem. Eng.*, 29, 1401–1409.

Gao, W., Hernandez, R., and Engell, S. (2016a). A study of explorative moves during modifier adaptation with quadratic approximation. *Processes*, 4(45). doi: 10.3390/pr4040045.

Gao, W., Hernandez, R., and Engell, S. (2017). Real-time optimization of a novel hydroformylation process by using transient measurements in modifier adaptation. In *IFAC-PapersOnLine*, volume 50, 5731–5736.

Gao, W., Wenzel, S., and Engell, S. (2016b). A reliable modifier-adaptation strategy for real-time optimization. *Comput. Chem. Eng.*, 91, 318–328.

Hentschel, B., Kiedorf, G., Gerlach, M., Hamel, C., Siedel-Morgenstern, A., Freund, H., and Sundmacher, K. (2015). Model-based identification and experimental validation of the optimal reaction route for the hydroformylation of 1- dodecene. *Ind. Eng. Chem. Res.*, 54, 1755–1765.

Hernandez, R. and Engell, S. (2016). Modelling and iterative real-time optimization of a homogeneously catalyzed hydroformylation process. In *Computer Aided Chemical Engineering*, volume 38, 1–6.

Kiedorf, G., Hoang, D., Mueller, A., Joerke, A., Markert, J., Arellano-Garcia, H., Siedel-Morgenstern, A., and Hamel, C. (2014). Kinetics of 1-dodecene hydroformylation in a thermomorphic solvent system using rhodium-biphosphos catalyst. *Chem. Eng. Sci.*, 115, 31–48.

Korpela, T., Suominen, O., Majanne, Y., Laukkanen, V., and Lautala, P. (2016). Robust data reconciliation of combustion variables in multi-fuel fired industrial boilers. *Control Eng. Pract.*, 55, 101–115.

Marchetti, A., Chachuat, B., and Bonvin, D. (2010). A dual modifier-adaptation approach for real-time optimization. *J. Process Control*, 20(9).

Marchetti, A., Francois, G., Faulwasser, T., and Bonvin, D. (2016). Modifier adaptation for real-time optimization - methods and applications. *Processes*, 4(55). doi: 10.3390/pr4040055.

Navia, D., Briceo, L., and de Prada, C. (2015). Modifier-adaptation methodology for real-time optimization reformulated as a nested optimization problem. *Ind. Eng. Chem. Res.*, 54, 12054–12071.

Roberts, P. (1979). An algorithm for steady-state system optimization and parameter-estimation. *Int. J. Syst. Sci.*, 10, 719–734.

Tatjewski, P. (2002). Iterative optimizing set-point control- the basic principle redesigned. In *15th Triennial World Congress IFAC*.

Zagajewski, M., Behr, A., Sasse, P., and Wittman, J. (2014). Continuously operated miniplant for the rhodium catalyzed hydroformylation of 1-dodecene in a thermomorphic multicomponent solvent system (TMS). *Chem. Eng. Sci.*, 115, 88–94.